Molecular Crystals and Liquid Crystals

Publication details, including instructions for authors and subscription information:
http://www.tandfonline.com/loi/gmcl20

Ultrafast Optical Nonlinearity in Polydiacetylenes Studied by Sub-5-fs Laser

Takayoshi Kobayashi [a] & Mitsuhiro Ikuta [a]

[a] Department of Physics, University of Tokyo, Bunkyo, Tokyo, Japan

Version of record first published: 16 Aug 2006

To cite this article: Takayoshi Kobayashi & Mitsuhiro Ikuta (2006): Ultrafast Optical Nonlinearity in Polydiacetylenes Studied by Sub-5-fs Laser, Molecular Crystals and Liquid Crystals, 446:1, 193-207

To link to this article: http://dx.doi.org/10.1080/15421400500374815

Mol. Cryst. Liq. Cryst., Vol. 446, pp. 193–207, 2006

ISSN: 1542-1406 print/1563-5287 online
DOI: 10.1080/15421400500374815

Taylor & Francis
Taylor & Francis Group

Ultrafast Optical Nonlinearity in Polydiacetylenes Studied by Sub-5-fs Laser

Takayoshi Kobayashi
Mitsuhiro Ikuta
Department of Physics, University of Tokyo, Bunkyo, Tokyo, Japan

Molecular vibration of several modes in blue-phase polydiacetylene-3-butoxycarbonylmethylurethane (PDA-3BCMU) was real-time observed by 5-fs pump-probe measurement. The contribution of the vibrational wavepackets in the ground state and in the excited state in the signal were separated by multichannel measurements The C=C stretching mode in the ground state starts to oscillate π-out-of-phase with the C≡C stretching mode. The structure of PDA-3BCMU in the geometrically relaxed state is not pure butatriene-type but more like acetylene-type. The frequencies of C=C and C≡C stretching modes there were determined by singular value decomposition method to be $1472 \pm 6\,cm^{-1}$ *and* $2092 \pm 6\,cm^{-1}$*, respectively. The double and triple bond stretching frequencies in the ground state which are* $1463 \pm 6\,cm^{-1}$ *and* $2083 \pm 6\,cm^{-1}$*, respectively.*

Keywords: Ag state; Bu state; C-C stretching mode; conjugated polymer; exciton; free excition; fs spectroscopy; geometrical relaxation; polydiacetylene; self-trapped exciton; wavepacket

1. INTRODUCTION

Due to the expanding demand for the high-density communication various research fields related to electronics, optoelectronics, and photonics are growing. In order to realize such technologies the optical devices and materials needed for the construction of such devices are being required and hence materials research targeting such applications

This research is supported partly by the Grant-in-Aid for Specially Promoted Research (#14002003) from the Ministry of Education, Science and Culture and also partly by the program for the "Promotion of Leading Researches" in Special Coordination Funds for Promoting Science and Technology from the Ministry of Education, Science and Culture.

Address correspondence to T. Kobayashi, Department of Physics, University of Tokyo, Hongo 7-3-1, Bunkyo, Tokyo 113-0033, Japan. E-mail: kobayashi@phys.s.u-tokyo.ac.jp

is developed with increasing speed. For such purposes optical and electrical properties, conjugated polymers have been attracting many scientists because of their many excellent properties [1,2]. The examples are flexible conductors, light-emitting diodes, and all-optical switches.

The polymers are of interest not only because of the above technological applications but also of fundamental physics since they have large and often ultrafast optical nonlinearities and are model materials of one-dimensional system with outstanding characteristic features including excitonic spectrum and ultrafast relaxation studied by spectroscopy. These features are deeply related to the formation of localized nonlinear excitations such as solitons, polarons, and a self-trapped exciton (STE) formed via a strong coupling between electronic excitations and lattice vibrations. Here we are utilizing the term STE in a sense that the geometrical relaxation takes place just after photoexcitation to form the STE. STE is sometimes called exciton polaron or neutral bipolaron eve though there is sometimes argument about the differences in their properties [3–16].

Among many polymers including conjugated and non-conjugated polymers polydiacetylenes (PDAs) have special interests, because PDAs have several phases named according to their colors and also they can have various morphologies, i.e., single crystals, solutions, and various films such as cast films, Langmuir films, and spin-coated films [17–20]. The ultrafast optical responses in PDAs have been intensively investigated by femtosecond time-resolved pump-probe spectroscopy and picosecond to femtosecond time-resolved Raman spectroscopy [2,6,10,11,21–30].

From previous extensive studies, [2,6,10,11,21–30] the initial changes in electronic absorption spectra and their ultrafast dynamics in a femtosecond region after photoexcitation of polydiacetylene (PDA) are explained in terms of the geometrical relaxation (GR) of a free exciton (FE) to a STE within 100 fs [2]. The STE is well established to be a geometrically relaxed state with admixture of butatriene-type configuration $(-CR{=}C{=}C{=}CR'-)_n$ from an acetylene-type chain $(=CR-C{\equiv}C-CR'-)_n$ [21,22] the substituted side groups R and R′ represent attached to the main chain. All of the stretching vibrations of carbon atoms are considered to be coupled to the photogenerated FE and induce various nonlinear optical processes different from those in most of inorganic semiconductors [10–13,28,31]. Experimental and theoretical studies have revealed that the lowest excited singlet state in a blue-phase PDA to be an optically forbidden 2^1A_g state lying $\sim$0.1 eV below an allowed 1^1B_u-FE state, which provides characteristic intense blue color which gives the name [3,32–36]. The internal conversion (IC) is then expected to take place along with self-trapping, [12,13] but the dynamical processes of IC and GR have not yet been

fully characterized [12,13]. Recent progress in femtosecond pulsed lasers has enabled to investigate molecular dynamics on a 10-fs timescale [23,24]. In the previous works, a wavepacket motion of C=C stretching mode with a period of ~23 fs was found in the photon-echo and transient bleaching signals of PDA-DCAD (poly(1,6-di(*n*-carbazolyl)-2,4 hexadiyne)) films by using 9–10 fs pulses [21,22]. This paper claimed that the CC double bond stretching appear just after excitation. While on the other the triple bond stretching does not appear and starts to grow sometime after while the time constant of the formation of the mode was not able to be determined.

The real-time observation of the geometrical relaxation in PDA has been enabled by the recent development of sub-5-fs visible pulse generation based on non-collinear optical parametric amplification (NOPA) system which satisfies all of the pulse-front matching, phase matching, and group-velocity matching conditions [37–39]. Utilizing compressors such as prism pair, grating pair, chirped mirror, and deformable mirror the shortest visible – near infrared pulse were obtained [37,39]. The trace of the delay-time dependence of the normalized difference transmittance $\Delta T(t)/T$ induced by a ultrashort pump pulse is called 'real-time spectrum'. It means a spectrum in a time domain namely the signal intensity plotted against the probe delay time. By time-resolved analysis of the Fourier transform of the real-time spectrum, the dynamic features of self-trapping, IC, and coupling between stretching and bending modes in the relaxed state in a PDA have been elucidated using sub-5 fs pulses in our previous study [30].

However these experiments have a remaining problem of the ambiguity in the assignment of the origins of the pump-probe signal traces to either the ground state or to an excited-state, because the ultrashort laser pulse with a wide enough spectrum can drive the coherent vibrations in both ground-states and excited states. In other word the short pulse with shorter duration time than the vibrational period drives the molecular vibration in the ensemble of molecules impulsively resulting in the synchronous oscillation of the molecules in the ensemble irrespective whether they are in the ground or in the excited state.

This ambiguity of the assignment prevents us from the well defined discussion of the dynamics of the wavepacket after being photogenerated. In this study, we could attribute the origins of the oscillation signals in pump-probe traces either to the ground or to the excited state by utilizing precise multi-channel detection method.

2. EXPERIMENTAL

The sample used in the present study is a cast film of blue-phase PDA-3BCMU (poly[4,6-docadiyn-1, 10-diolbis (*n*-butoxycarbonyl-

methylurethane)]) on a glass substrate. PDA-3BCMU has side groups of $R = R' = -(CH_2)_3OCONHCH_2COO(CH_2)_3CH_3$, in the backbone chain structure of $(=RC-C\equiv C-CR'=)_n$. PDA-3BCMU is one of the well-known soluble PDAs. The laser pulses for both pump and probe are produced by NOPA seeded by a white-light continuum with a 5-fs pulse compressor system [29,39–41]. The source of this system is a commercially supplied regenerative amplifier (Spectra-Physics, model Spitfire), of which pulse duration, central wavelength, repetition rate, and average output power are 100 fs, 790 nm, 5 kHz, and 800 mW, respectively. The spectrum of the pump and probe pulses covers a spectral range from 520 to 730 nm with a nearly constant phase providing a Fourier transformed temporal shape. Laser pulse energies of the pump and probe pulses are about 35 and 5 nJ, respectively. Time trace of normalized difference transmittance ($\Delta T(t)/T$) was obtained as a function of pump-probe delay-time (t) from –100 to 1200 fs with every 1-fs step. Simultaneous measurement was performed by a multi-channel lock-in amplifier designed by EG&G over the spectral range extending from 540 to 740 nm using a 300 grooves/mm grating monochromator with spectral resolution of about 3.6 nm. All the measurements were performed at room temperature (295 ± 1 K).

3. RESULTS AND DISCUSSION

Figure 1 shows the observed the normalized difference transmittance $\Delta T(t)/T$ of the blue-phase PDA-3BCMU sample displayed two dimensionally (probe-photon energy *versus* probe delay time). Figure 2 exhibits several examples of $\Delta T(t)/T$ traces at several energies of probe photon. All of the traces have signals of finite size at negative delay times and sharp and intense peaks around zero probe-delay time. The former is due to the perturbed free induction decay process associated with the third-order nonlinearity of the sequential interaction of probe-pump-pump fields modified with molecular vibrations. The latter signals are due to pump-probe coupling induced by the nonlinear process of the pump-probe-pump time ordering. There is another contribution from the interference between the scattered pulses and the probe pulses of which duration are elongated in the monochromator. The details of the vibrational modulation observed at longer delay times than about 50 fs are free from the distortions induced by the above-mentioned two mechanisms.

Figure 3 shows the measured normalized difference transmittance spectra at a few probe delay times. In the probe-photon energy region above 1.95 eV the normalized difference transmittance is positive because of photobleaching of the 1^1B_u-FE absorption peaked around

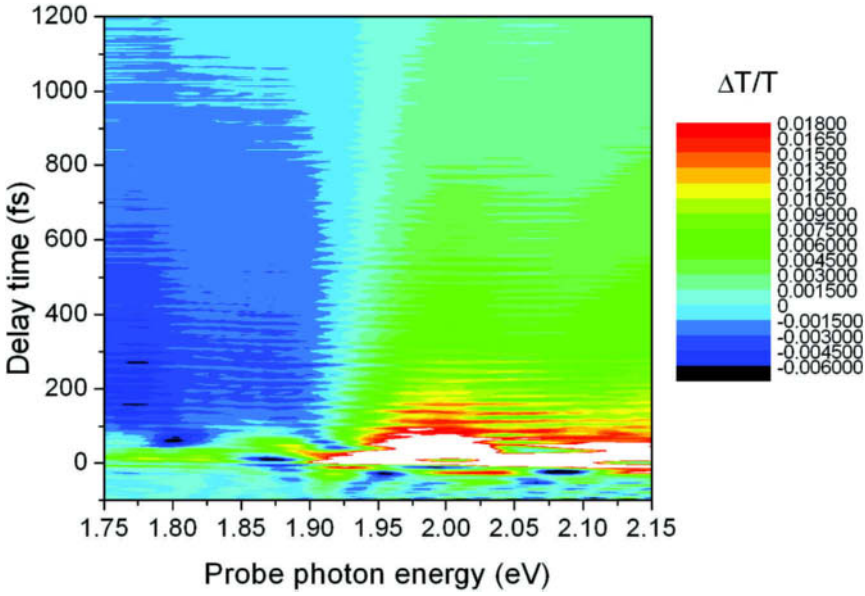

FIGURE 1 Two-dimensional normalized difference transmittance ($\Delta T(t)/T$). The signal intensity is plotted against both the probe-photon energy (abscissa) and probe delay time (ordinate).

2.0 eV. In the probe-photon energy region below 1.90 eV the normalized difference transmittance signals are negative due to the photoinduced transition from the geometrically relaxed 2^1A_g state to the higher excited nB_u state which is one of the four essential states [30,42]. The 1^1B_u-FE state decays within 100 fs into the geometrically relaxed 2^1A_g state [2,31,43].

The power spectrum of Fourier transform of $\Delta T(t)/T$ at 128 probe-photon energies probed by using the multi-channel lock-in amplifier is shown in Figure 4. For the calculation the signal data in the probe delay time ranging from 400 to 900 fs were used after high-pass step-function filtering with a threshold frequency of 1,000 cm^{-1}. In the wide range of probe-photon energy, three peaks were observed at 1,220, 1,460, and 2,080 cm^{-1} corresponding to the C−C, C=C, and C≡C stretching modes, respectively [44–46]. The probe-photon energy dependences of the Fourier power of these modes are shown in Figure 5. All of the three modes have peaks around 1.78, 1.95, and 2.05 eV in common.

In order to investigate more deeply the dynamics of the vibrational modes excited by the ultrashort pulse laser in the polymer system, we

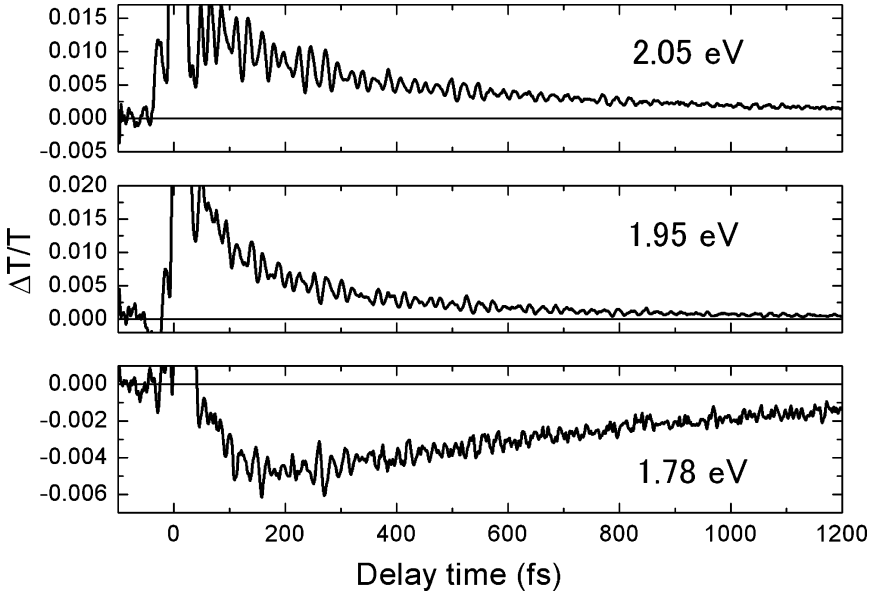

FIGURE 2 Pump-probe delay time dependence of the normalized difference transmittance ($\Delta T(t)/T$) on the probe delay time at three probe photon energies.

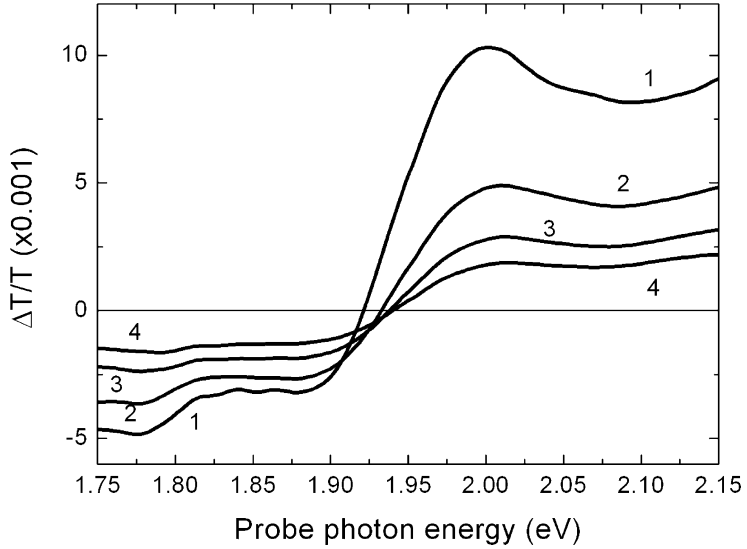

FIGURE 3 Normalized difference transmittance spectra ($\Delta T/T$); 1, delay at 200 fs; 2, 500 fs; 3, 800 fs; 4, 1100 fs.

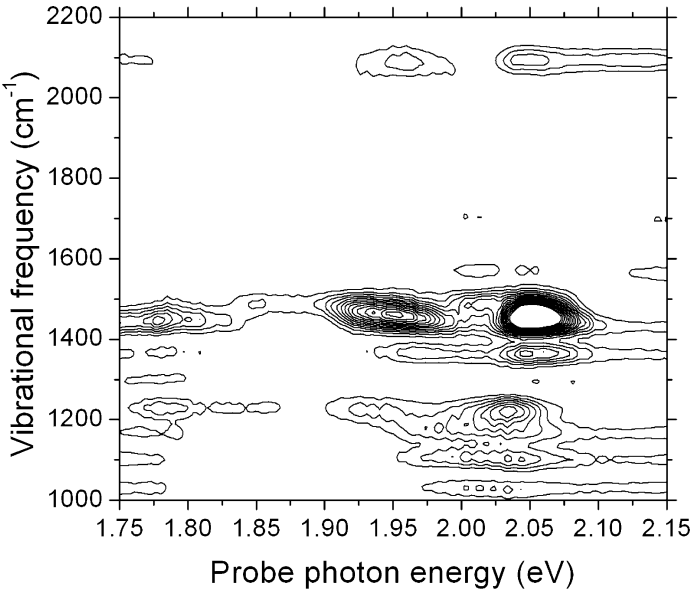

FIGURE 4 Two-dimensional Fourier power spectra of the $\Delta T/T$ traces. The signal intensity is plotted against both the probe-photon energy (abscissa) and probe the vibration frequency (ordinate).

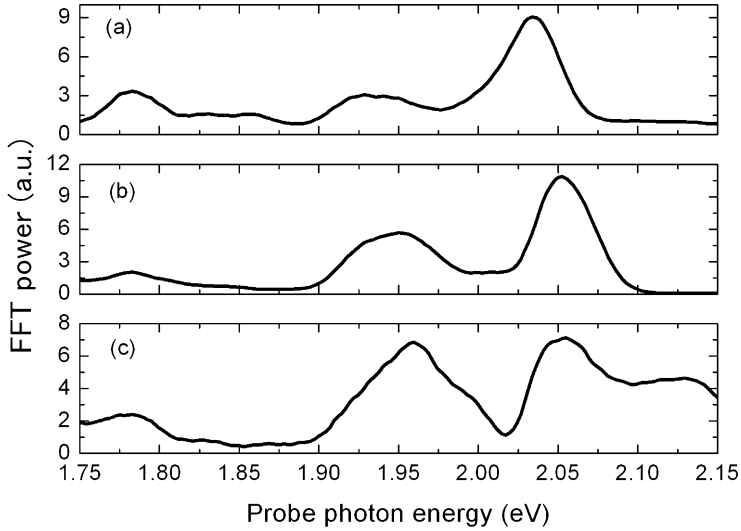

FIGURE 5 Fast Fourier Power spectra of the modes of (a), C−C; (b), C=C; and (c), C≡C stretching extracted from the $\Delta T/T$ traces.

analyzed the pump-probe signal by a linear prediction singular value decomposition (LP-SVD) method, which is most efficiently and precise utilized when many spectral components can be obtained simultaneously as in the present case by invoking a global fitting method to be discussed later. By LP-SVD, single or multiple mode(s) of damped oscillation were extracted from the data such as $y(t) = A \exp(-t/\tau) \cos(\Omega t + \theta)$, where A is an initial amplitude of the signal modulation of $\Delta T(t)/T$ due to molecular vibration, τ is the decay time, Ω is the mode frequency, and θ is the initial phase. These value of each vibrational mode of C−C, C=C, and C≡C was extracted by the LP-SVD method from the 200–900 fs data after rectangular frequency filtering of the Fourier power spectrum (1,150–1,290, 1,395–1,535, and 2,010–2,150 cm^{-1}) at each probe-photon energy independently. The amplitude at 300 fs of each mode is shown in Figure 6. The spectrum of amplitude of C−C stretching mode in Figure 6(a) does not resemble the FFT-power spectrum of C−C mode in Figure 5(a). The vibration signal of C−C stretching mode was not strong enough for the mode signal to be extracted out from the real-time data to be analyzed to obtain its decay time and initial phase with enough preciseness. Hereafter we will concentrate on the pump-probe signal of only C=C and C≡C stretching modes extracted by LP-SVD.

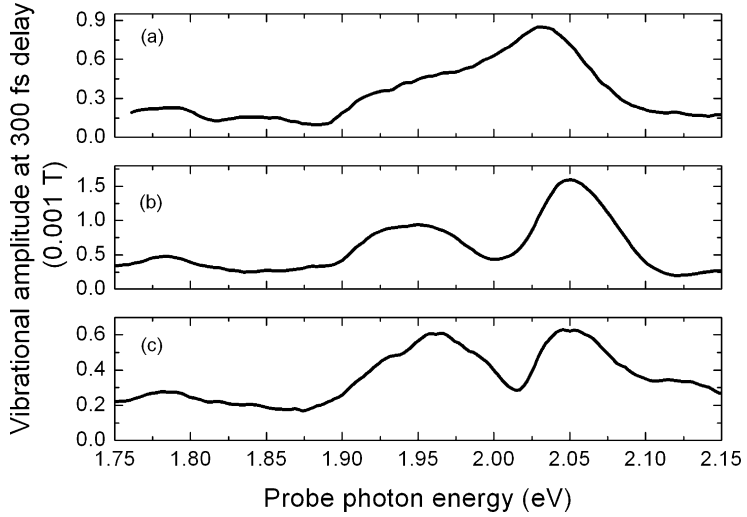

FIGURE 6 Fourier amplitude at the probe delay of 300 fs extracted from the normalized difference transmittance by the method of LP-SVD for the modes of (a), C−C; (b), C=C; and (c), C≡C stretching.

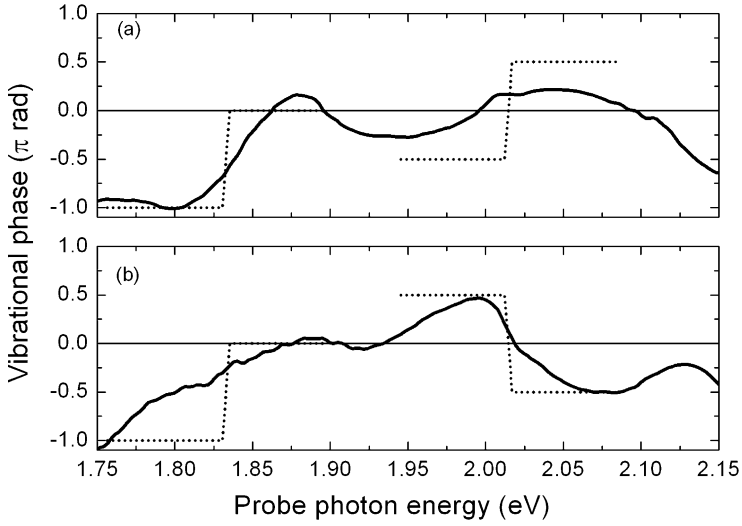

FIGURE 7 Initial phase (solid curve) of each vibrational mode of normalized difference transmittance by the method of LP-SVD for the modes of (a), C=C; and (b), C=C stretching. The expected phase (dotted line) of vibration from the model of the wavepacket motion in the ground state (1.95–2.07 eV) and in the excited state (1.76–1.88 eV).

The absolute initial phases of the C≡C and C≡C modes are both shown in Figure 7. In order to explain the features of the phase spectra in Figure 7, a simple model are proposed in the following way. In Figure 8(a) and (c), transition from the ground state to 1^1B_u-FE state and that from the geometrically relaxed 2^1A_g state to a higher excited n^1B_u state, respectively, are represented on the potential curves of PDA. The FWHM of pulse of the NOPA output used as a pump is much shorter than the oscillation periods of C=C 23 fs and C≡C vibrations 16 fs. Therefore it can generate vibrational wavepackets impulsively in the ground state and/or 1^1B_u-FE state. The wavepacket in the ground state is made at point B in Figure 8(a), which is located at the bottom of potential curve surface of the ground state, and it begins to oscillate on the potential curve as $B \rightarrow A \rightarrow B \rightarrow C \rightarrow B \cdots$ (or $B \rightarrow C \rightarrow B \rightarrow A \rightarrow B \ldots$). After the wavepacket is generated, absorption intensity increases when the wavepacket is located at the probe-photon frequency that is corresponding to the vertical transition energy at the position of the wavepacket. Therefore the oscillation of wavepacket results in the modulation of normalized difference transmittance with the vibrational frequency.

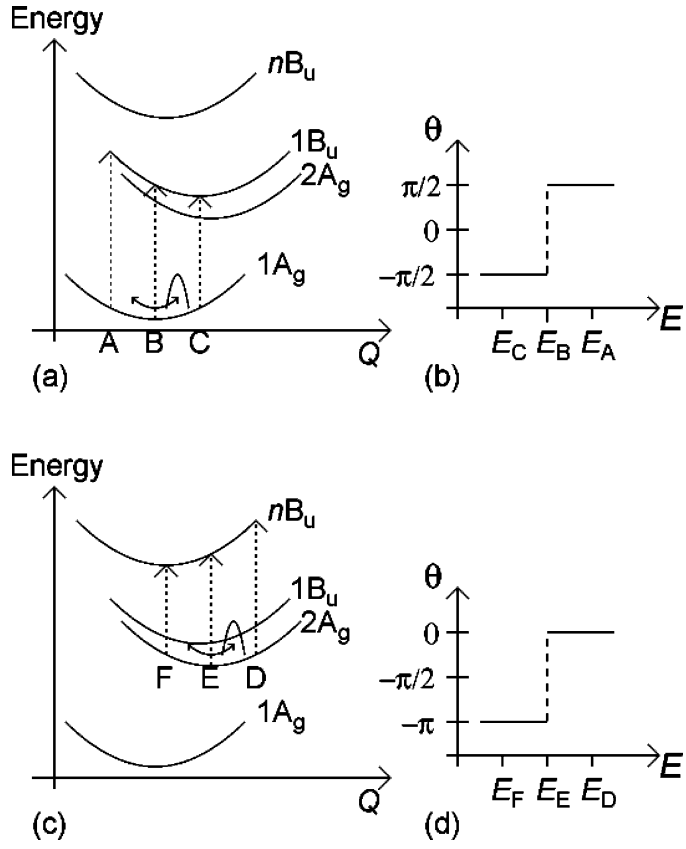

FIGURE 8 (a) Transition from the ground states on potential energy curves of PDA. Point B is located at the bottom of the potential curve of the ground states. (b) The model phase of vibration by the motion of the wavepacket in the ground state. E_X is the energy of transition from position X. (c) Transition from the excited states on potential energy diagram of PDA. Point E is located at the bottom of the curve of the ground states. (d) The model phase of vibration by the motion of the wavepacket in the excited state.

If the wavepacket photoproduced at B starts to oscillate as described by $B \rightarrow A \rightarrow B \rightarrow \cdots$, the transmittance at probe photon energy E_A starts to decrease initially, and at the same time the transmittance at E_C starts to increase. Here E_X is the transition energy from position X (=A, B, C, D, E, or F) on the lower state to the upper state. In this case the phase of the vibration of $\Delta T(t)/T$ is $\pi/2$ at probe photon energy higher than E_B, and $-\pi/2$ at that lower than E_B as

shown in Figure 8(b). If the wavepacket starts to move to the reverse direction ($B \rightarrow C \rightarrow B \rightarrow \ldots$), the phase is $-\pi/2$ for the probe-photon energy higher than E_B, and $\pi/2$ at that lower than E_B.

Figure 7(a) shows that the phases determined for the C=C stretching mode from about 1.9 to 2.0 eV are negative while those between about 2.0 and 2.1 eV are positive. These features can be explained using Figure 8(a) and (b) where E_B is 2.0 eV, which corresponds to the 1^1B_u-FE absorption peak. The phase of the C=C stretching mode at 2.02 eV is positive, while that of the C≡C stretching mode at 2.02 eV in Figure 7(b) is close to zero. This energy (2.02 eV) corresponds to the photon energy shifted by the C=C stretching energy (0.18 eV) from 2.2 eV of the peak of the probe which is expected to give a $\pi/2$ phase. Therefore it can be concluded that the phases of the C=C stretching mode around 2.02 eV are shifted to positive due to the contribution of the Raman gain signal which is expected to appear from the energy difference between the peak of the pump laser and the energy corresponding to the C=C stretching mode frequency. The phases of C≡C stretching are positive from about 1.93 to 2.02 eV and are negative between about 2.02 and 2.15 eV. Form this phase relation it can be concluded that the wavepacket of C≡C mode generated on the ground-state potential curve starts to move to the reverse direction to that of the C=C stretching mode.

The phases of C=C mode around 1.95 eV and 2.05 eV are neither $\pi/2$ nor $-\pi/2$. It can be explained in the following way. Intense signal of photoinduced absorption modulated by the wavepacket of C=C mode in the excited state is expected also to be generated appear relatively strongly in the photon energy region. Then the phases of C=C mode are considered to be zero as expected for a wavepacket in the excited state. Because of the overlap of the vibrational signals due to the ground state and to the excited state with nearly the same frequencies the observed values of the phases are expected to correspond to the weighted averages of the two contributions. The frequency difference between the ground state and the excited state is expected to be smaller than 10 cm^{-1}, which correspond to about 1% of the mode frequency from the vibrational frequency data of various molecular systems. Therefore the difference becomes clear after several tens oscillation period of the mode namely about 1 ps after excitation.

From the experimental results of the phases at 1.95 and 2.05 eV having an opposite sign to each other, it can be concluded that the vibrational-amplitude peaks at 1.95 and 2.05 eV are due to the modulation of the intensity of 1^1B_u-FE absorption (resonant at 2.00 eV) by the motion of the vibrational wavepacket induced by the stimulated Raman scattering (SRS) process in the ground state.

Figure 8(c) represents the diagram of photoinduced absorption from the geometrically relaxed 2^1A_g state. The pump pulse makes wavepackets not only in the ground state but also in the 1^1B_u-FE state. The wavepacket photoexcited in the 1^1B_u-FE state soon (< 100 fs) after generation relaxes into the geometrically relaxed 2^1A_gstate. In our group we found that this relaxation time was determined to be 60 ± 20 fs [47]. The oscillation of the wavepacket on the geometrically relaxed 2^1A_g state potential curve modulates the probe signal. A wavepacket is produced at point F in Figure 8(c) at the beginning, and then makes a start to move as F→E→D→E→F . . ., where point E is located at the bottom of the geometrically relaxed 2^1A_g state potential curve along the corresponding stretching-mode coordinate.

The expected phases of the oscillation of the photoinduced-absorption signal in the case of $E_D > E_F$ are shown in Figure 8(b), i.e., they are zero, $-\pi/2$, and $-\pi$ at E_D, E_E, and E_F, respectively, on the analogy of the ground-state.

The spectrum of absorption from the geometrically relaxed 2^1A_g state to n^1B_u states has a peak around 1.8 eV.[28] If E_E is 1.83 eV, the phases of the C=C mode in Figure 7(a) correspond to the model phase in Figure 8(d). The phases of C≡C mode at 1.77 and 1.87 eV are $-\pi$ and zero, respectively, in the same way as the phases of C=C mode. Therefore it is concluded that not only the vibrational wavepacket of C=C mode but also that of C≡C mode is also generated in the geometrically relaxed 2^1A_g state. This clearly demonstrates that the full geometrically relaxed butatriene-type structure is not formed, but it can still be described in the form of acetylene-type structure, as discussed previously by one of the present authors [30].

Figure 9 shows that the frequencies of C=C mode at 128 probe-photon energies extracted by LP-SVD from the real-time traces. From the previous discussion, the signal due to the wavepacket motion in the ground state appears strongly at the probe-photon energies of 2.04–2.07 eV and 1.92–1.95 eV, which correspond to E_A and E_C, respectively in Figure 8. The oscillatory motion of the wavepacket in the geometrically relaxed 2^1A_g state appears strongly at the probe-photon energies of 1.87–1.90 eV and 1.79–1.81 eV, indicated by E_D and E_F regions in the Figure. At the probe-photon energies of 2.00 eV and 1.84 eV, which are marked with E_B and E_E, respectively, the vibration of wavepacket in the geometrically relaxed 2^1A_g state and that of the ground state, respectively, appear nearly exclusively. Figure 9 shows that the vibrational frequencies determined for the probe photon energies of E_B, E_D, and E_F are higher than those of E_A, E_C, and E_E. Hence it can be concluded that the frequency of C=C stretching in the geometrically relaxed 2^1A_g state is close to that

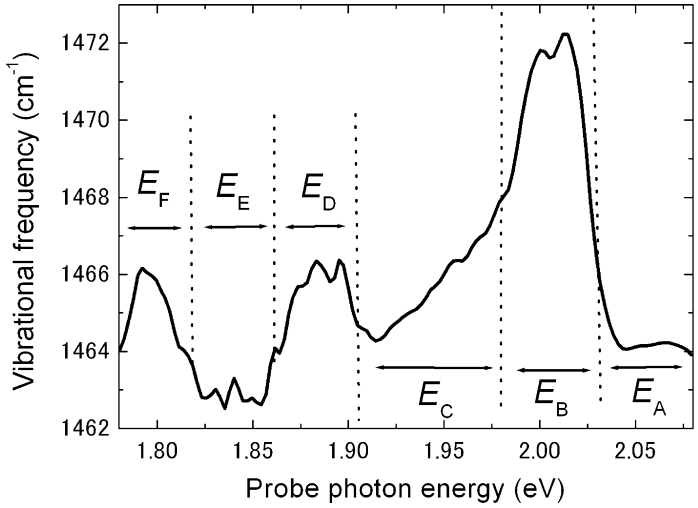

FIGURE 9 The probe photon energy dependence of vibrational frequency of C=C stretching mode. E_A and E_C are energy regions in which the pump-probe signal is modulated by the motion of the wavepacket in the ground state strongly rather than the excited state. E_D and E_F are energy regions in which the pump-probe signal is modulated by the motion of the wavepacket in the ground state strongly rather than the excited state. In E_B and E_E, the signal is modulated by the motion of the wavepacket only in the excited/ground state, respectively.

determined for E_B probe photon energy. Therefore the frequency of the C=C stretching in the excited state is concluded to be $1472 \pm 6\,\text{cm}^{-1}$ and that in the ground state which is $1463 \pm 6\,\text{cm}^{-1}$ concluded for E_E probe photon energy. The frequency of C≡C stretching mode in the geometrically relaxed 2^1A_g state is determined to be $2092 \pm 6\,\text{cm}^{-1}$, while that in the ground state is $2083 \pm 6\,\text{cm}^{-1}$. The errors of the differences are smaller than those of their absolute values, since the errors in the frequency determination are mainly due to the imperfect step length of the delay stage. It can then be concluded that each of the frequencies of the C=C and C≡C stretching in the excited state is higher by about $10 \pm 2\,\text{cm}^{-1}$ than each of those in the ground state.

4. CONCLUSION

In conclusion, we separated the ground state and the excited-state contributions in the real-time vibrational signals due to the wavepacket motions from the difference transmittance spectra obtained

by multi-wavelength sub-5 fs spectroscopy. The wavepacket of C=C stretching mode in the ground state was found to start at first to oscillate to the *opposite* direction to that of C≡C stretching mode. Also the vibration of C≡C stretching mode in the geometrically relaxed 2^1A_g state was observed as well as C=C mode even after the FE is converted to the geometrically relaxed state within 100 fs. The frequencies of C=C and C≡C stretching modes in the geometrically relaxed 2^1A_g state were determined to be 1472 and 2092 cm^{-1}, respectively. The corresponding frequencies in the ground state were calculated as 1463 and 2083 cm^{-1}. Each of the formers is higher by about 10 cm^{-1} than each of the latter.

REFERENCES

[1] Kobayashi, T. (1992). *IEICE Trans. Fundam.*, *E-75A*, 38.
[2] Yoshizawa, M., Hattori, Y., & Kobayashi, T. (1993). *Phys. Rev. B*, *47*, 3882.
[3] Heeger, A. J., Kivelson, S., Schrieffer, J. R., & Su, W. P. (1988). *Rev. Mod. Phys.*, *60*, 781.
[4] Su, W. P., Schrieffer, J. R., & Heeger, A. J. (1979). *Phys. Rev. Lett.*, *42*, 1698.
[5] Su, W. P., Schrieffer, J. R., & Heeger, A. J. (1980). *Phys. Rev. B*, *22*, 2099.
[6] Yoshizawa, M., Kobayashi, T., Fujimoto, H., & Tanaka, J. (1982). *J. Phys. Soc. Jpn.*, *56*, 338.
[7] Vardeny, Z. (1984). *Physica*, *127B*, 338.
[8] Rothberg, L., Jedju, T. M., Etemad, S., & Baker, G. L. (1985). *Phys. Rev. Lett.*, *57*, 3229.
[9] Greene, B. I., Mueller, J. F., Orenstein, J., Rapkine, D. H., Schmitt-Rink, S., & Thakur, M. (1988). *Phys. Rev. Lett.*, *61*, 325.
[10] Kobayashi, T., Yoshizawa, M., Stamm, U., Taiji, M., & Hasegawa, M. (1990). *J. Opt. Soc. Am. B*, *7*, 1558.
[11] Yoshizawa, M., Nishiyama, K., & Kobayashi, T. (1993). *Chem. Phys. Lett.*, *207*, 461.
[12] Kobayashi, T., Yasuda, M., Okada, S., Matsuda, H., & Nakanishi, H. (1997). *Chem. Phys. Lett.*, *267*, 472.
[13] Kinugusa, J., Shimada, S., Matsuda, H., Nakanishi, H., & Kobayashi, T. (1998). *Chem. Phys. Lett.*, *287*, 639.
[14] Zerbetto, F. (1994). *J. Phys. Chem.*, *98*, 13157.
[15] Swiatkiewicz, J., Mi, X., Chopra, P., & Prasad, P. N. (1987). *J. Chem. Phys.*, *87*, 1882.
[16] Zheng, L. X., Benner, R. E., Vardeny, Z. V., & Baker, G. L. (1992). Synth. *Metals*, *49/50*, 313.
[17] Wegner, G. (1971). *Makromol. Chem.*, *145*, 85.
[18] Patel, G. N., Chance, R. R., & Witt, J. D. (1979). *J. Chem. Phys.*, *70*, 4387.
[19] Bloor, D. (1985). In: *Polydiacetylenes*, Bloor, D. & Chance, R. R. (Eds.), Martinus Nijhoff Publishers: Dordrecht, Netherlands.
[20] Tashiro, K., Ono, K., Minagawa, Y., Kobayashi, M., Kawai, T., & Yoshino, K. (1991). *J. Polym. Sci., Part B*: *Polym. Phys.*, *29*, 1223.
[21] Bigot, J. Y., Pham, T. A., & Barisien, T. (1996). *Chem. Phys. Lett.*, *259*, 469.
[22] Pham, T. A., Daunois, A., Merle, J. C., Le Moigne, J., & Bigot, J. Y. (1995). *Phys. Rev. Lett.*, *74*, 904.

[23] Wang, Q., Shoenlein, R. W., Petearnu, L. A., Mathies, R. A., & Shank, C. V. (1994). *Science*, *266*, 422.
[24] Cerullo, G., Lanzani, G., Muccini, M., Taliani, C., & De Silvestri, S. (1999). *Phys. Rev. Lett.*, *83*, 231.
[25] Vierheilig, A., Chen, T., Walther, P., Kiefer, W., Materny, A., & Zeweil, A. H. (1999). *Chem. Phys. Lett.*, *312*, 349.
[26] Yoshizawa, M., Taiji, M., & Kobayashi, T. (1989). *IEEE J. Quantum Electron*, *25*, 2532.
[27] Yoshizawa, M., Yasuda, A., & Kobayashi, T. (1991). *Appl. Phys. B*, *53*, 296.
[28] Yoshizawa, M., Hattori, Y., & Kobayashi, T. (1994). *Phys. Rev. B*, *49*, 13259.
[29] Shirakawa, A., Sakane, I., & Kobayashi, T. (1998). *Opt. Lett.*, *23*, 1292.
[30] Kobayashi, T., Shirakawa, A., Matsuzawa, H., & Nakanishi, H. (2000). *Chem. Phys. Lett.*, *321*, 385.
[31] Yoshizawa, M., Kubo, A., & Saikan, S. (1999). *Phys. Rev. B*, *60*, 15632.
[32] Su, W. P., Schrieffer, J. R., & Heeger, A. J. (1980). *Phys. Rev. B*, *22*, 2099.
[33] Su, W. P., Schrieffer, J. R., & Heeger, A. J. (1982). *Phys. Rev. Lett.*, *68*, 1148.
[34] Abe, S., Yu, J., & Su, W. P. (1992). *Phys. Rev. B*, *45*, 8264.
[35] Abe, S., Schreiber, M., Su, W. P., & Yu, J. (1992). *Phys. Rev. B*, *45*, 9432.
[36] Pakbaz, K., Lee, C. H., Heeger, A. J., Hagler, T. W., & McBranch, D. (1994). *Synthetic Met.*, *64*, 295.
[37] Shirakawa, A. & Kobayashi, T. (1998). *Appl. Phys. Lett.*, *72*, 1476.
[38] Cerullo, G., Nisoli, M., Stagira, S., De Silvestri, S., Tempea, G., Krausz, F., & Ferencz, K. (2000). *Appl. Phys. B*, *70*, s253.
[39] Baltuška, A. & Kobayashi, T. (2002). *Appl. Phys. B*, *75*, 427.
[40] Shirakawa, A., Sakane, I., Takasaka, M., & Kobayashi, T. (1999). *Appl. Phys. Lett.*, *74*, 2268.
[41] Kobayashi, T. & Shirakawa, A. (2000). *Appl. Phys. B*, *70*, S239.
[42] Mazumdar, S., Guo, D., & Dixit, S. N. (1993). *Synthetic Met.*, *57*, 3881.
[43] Turki, M., Barisien, T., Bigot, J. Y., & Daniel, C. (2000). *J. Chem. Phys.*, *112*, 10526.
[44] Iqbal, Z., Chance, R. R., & Baughman, R. H. (1977). *J. Chem. Phys.*, *66*, 5520.
[45] Lewis, W. F. & Batchelder, D. N. (1979). *Chem. Phys. Lett.*, *60*, 232.
[46] Grando, D., Sottini, S., & Gabrielli, G. (1998). *Thin Solid Films*, *327–329*, 336.
[47] Yuasa, Y., Ikuta, M., Kimura, T., Matsuda, H., & Kobayashi, T. *Phys. Rev. B*, *72*, 134302.